Experimental Test Results for a Fiber Bragg Grating-based Flow Sensor

Robbert Pannekeet, Rodrigo Rodriguez-Erdmenger, Eric J. Ruggiero, Alexander Simpson and Christopher Wolfe

Journal of Intelligent Material Systems and Structures 2011 22: 1411 originally published online 1 August 2011
DOI: 10.1177/1045389X11414957

Experimental Test Results for a Fiber Bragg Grating-based Flow Sensor

Robbert Pannekeet,[1,*] Rodrigo Rodriguez-Erdmenger,[1] Eric J. Ruggiero,[2] Alexander Simpson[1] and Christopher Wolfe[2]

[1]*GE Global Research, Munich, Germany*

[2]*GE Global Research, Niskayuna, NY, USA*

ABSTRACT: A fiber optic-based mass flow sensor has been developed that uses fiber Bragg gratings to deduce flow velocity. Flow velocity, local temperature, pressure measurements (which all can be extracted using fiber Bragg gratings), and geometric information can be combined to determine mass flow.

A range of concepts have each been investigated and compared using the same "design of experiment" for each sensor. The most promising concept has been further developed into a prototype. The working prototype successfully demonstrated a thermally insensitive sensor design that has the capability to track flow velocities. The sensor design is incorporated directly with a structural beam element to magnify the strain effect while simultaneously compensating for thermally induced wavelength shifts in the sensor response. Further testing has been performed using three flexible beams at different angular positions, demonstrating that flow angles can be measured using a similar approach to that used for three-hole pneumatic probes. As a final test, the sensor has been tested in a shock tube, demonstrating superior performance to steady pneumatic measurements, which rely on tubing to reach the measurement location.

Key Words: fiber optic, bragg grating, FBG, mass flow, flow sensor, gas turbine.

INTRODUCTION

One of the key challenges facing power generation design engineers is the proper modeling of flow circuits throughout the gas turbine prior to releasing the product to market. Flows throughout the gas turbine influence key design parameters such as component life (via cooling flows) and combustion dynamics. From the system perspective, primary and secondary flows throughout the gas turbine play an important role in determining the overall cycle efficiency. The overall cycle efficiency can be increased when the secondary flows are characterized properly and reduced accordingly.

One possible sensor type that can be easily integrated into components is fiber Bragg grating (FBG) sensors (Udd, 1995; Hill and Meltz, 1997; Othonos, 1997; Rao, 1997). FBG sensors are coupled opto-mechanically, and thus provide a unique means of monitoring both thermally induced and mechanically induced strains using the same sensor (Botsis et al., 2005; Jin et al., 2006).

A fiber optic-based mass flow sensor can be used to deduce flow velocity. Flow velocity, local temperature, pressure measurements (which all can be extracted using fiber Bragg gratings) and geometric information can be combined to determine mass flow. The benefits of using fiber Bragg grating technology include:

1. high temperature survivability—fiber sensors are suitable for high-temperature operation;
2. frequency-based architecture—fiber Bragg gratings do not require an intensity measurement, making them immune to "dirty optic" and birefringence effects; and
3. redundancy—distributed sensor arrays can be designed to operate in transmission or reflection, adding built-in redundancy during field operation.

FLOW SENSOR CONCEPTS

As the flow velocity measurement was thought to be the most challenging feature to incorporate, it was decided to first investigate this type of measurement. Three prototypes were manufactured and tested on their performance with the open fiber probe, single sensor flexible beam probe and the differential flexible

*Author to whom correspondence should be addressed.
E-mail: pannekeet@research.ge.com
Figures 1–4 and 6–12 appear in color online: http://jim.sagepub.com

1045-389X/11/13 1411–7 $10.00/0 DOI: 10.1177/1045389X11414957

beam probe, respectively. The open fiber probe was rapid prototyped using stereolithography. In Figure 1 a schematic and a photograph of the open fiber are presented. The single sensor flexible beam and the differential flexible beam were cut from polymethylmethacrylate (PMMA) material and the sensors were attached to the body using a fast-acting adhesive. The differential set-up of a fiber Bragg has been demonstrated previously by Zhao et al. (2005). Figures 2 and 3 show schematics of the single sensor flexible beam and the differential flexible beam, respectively.

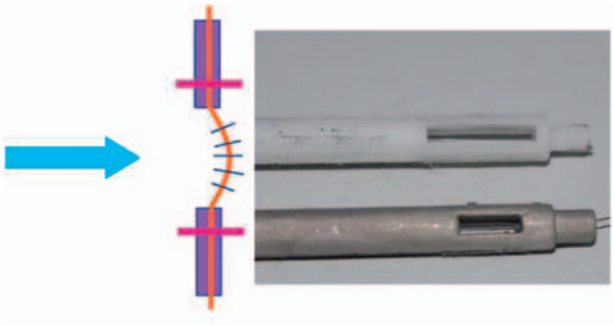

Figure 1. *Schematic and photo of the open fiber.*

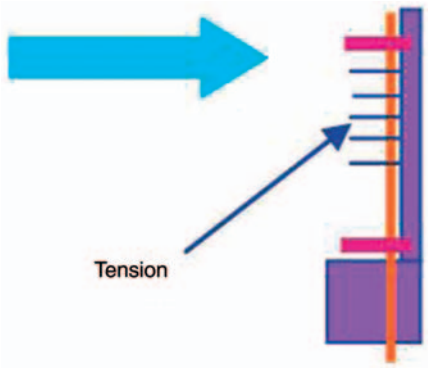

Figure 2. *Schematic of the single sensor beam.*

EXPERIMENTAL SET-UP

This section describes the experimental set-up used for performing the design of experiment (DOE) on the different designs discussed in the previous chapter. Firstly, the free stream jet will be described followed by the description of the DOE performed. Figure 4 shows a schematic of the experimental set-up on the left and a photograph of the air velocity calibrator (TSI 1128C) used to produce the free stream jet on the right.

The velocity calibrator is supplied with four nozzle configurations. This allows the user to optimize the accuracy of the velocity to the range required. For the experiments performed it was decided to use the nozzle for the range Mach 0.03–1. In the plenum of the velocity calibrator the pressure is measured with a US10000 absolute pressure transducer with a range of 17.4 pounds per square inch (psi) (1.2 bar) and an accuracy of ±0.05% of full scale. This results in an accuracy of ±0.5 m/s at a jet velocity of 328.1 feet/s (100 m/s), which is suitable for proof of concept of the designs.

The air supply used for the free stream jet is an inhouse system with a maximum pressure of 90 psi (6 bar) and is able to supply up to 0.22 pounds/s (100 g/s). Constant pressure at inlet of the velocity calibrator is regulated with a manual pressure regulator.

Temperature is measured at two locations: in the plenum of the velocity calibrator and at the exit of the nozzle. The plenum temperature controls the temperature (T_1) of the flow using an Omega CN8200 temperature and process controller in combination with a 400-watt Omega AHP in-line air heater. The jet temperature (T_2) is measured to calculate the exact speed of sound and to correlate the sensor response to temperature. At both locations *t*-type thermocouples with an accuracy of ±0.5°C are installed.

The probes are positioned 0.4 inch (10 mm) above and centered over the nozzle with an automated three-axis traverse system.

A Micron Optics SM130 optical sensor interrogator is the basis for the wavelength measurement. This system

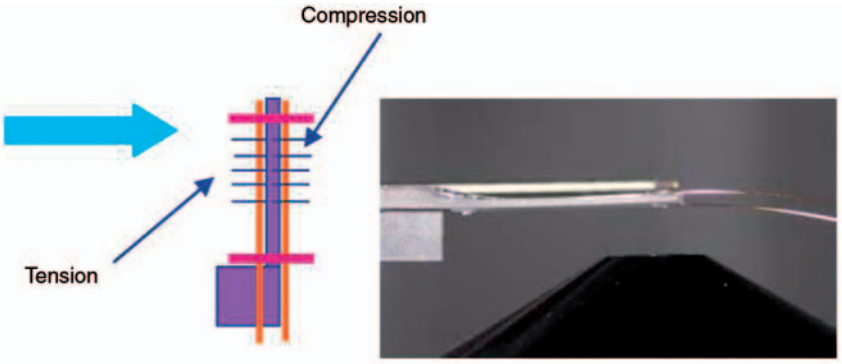

Figure 3. *Schematic and photo of the differential sensor beam.*

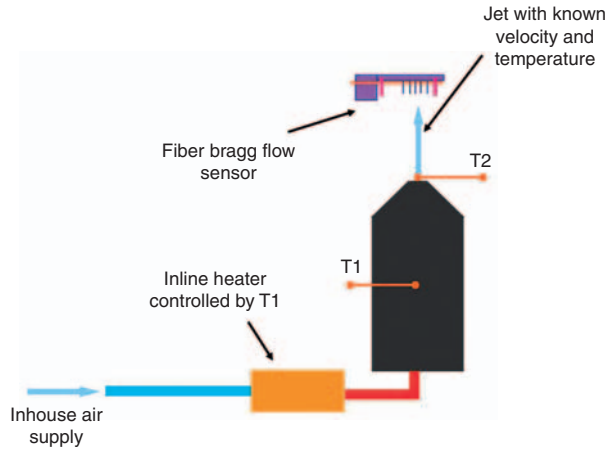

Figure 4. *Schematic of the experimental set-up.*

Table 1. Design of experiment.

	Velocity (m/s)	Temperature (K)
Data	64.5	299.4
	135.1	301.6
	66.2	309.4
	138.3	309.7
	150.1	305.1
	104.8	310.3
	52.6	305.3
	101.3	298.2
	103.2	303.8
Validation	140.6	310.2
	145.1	302.2
	81.8	298.3

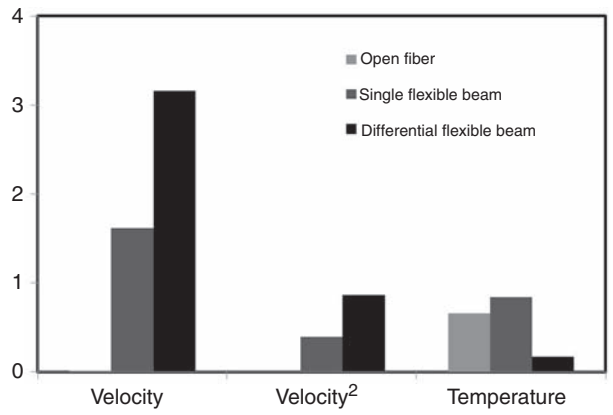

Figure 5. *Comparison of the three prototypes in a Pareto chart.*

acquires the sensor wavelength at 500 Hz with a repeatability of 1 microstrain.

DESIGN OF EXPERIMENT

To compare the different designs a "design of experiment" (DOE) was set up. The input parameters (Xs) were defined as velocity (range 160–500 ft/s [50–150 m/s]) and temperature (range 298–315 K). Temperature has been taken into account as it had been identified as a major factor in previous experiments. Sensor output in peak wavelength (nm) is defined as the output parameter (Y). An optimal DOE was chosen resulting in a nine-run central composite design (CCD) with three validation runs. Table 1 presents the DOE in metric units performed on all probe designs.

The designs were then compared using a Pareto effect chart showing the influence of the input parameters on the output parameter. The accuracy of the design was estimated by comparing the transfer function derived from the calibration runs with those derived from the validation runs.

For each point, steady state was required for 2 minutes; subsequently, the sensor output was measured for 7 minutes

RESULTS

A first comparison of the different concepts was based on the "Pareto chart." A Pareto chart visualizes the sensitivity of the output of the transfer function to the input parameters (velocity and temperature). Figure 5 presents a comparison between the three prototypes.

Open Fiber

The Pareto chart of the open fiber, with the left bar representing the velocity term, the middle bar the velocity squared term, and the right bar the temperature term in the transfer function. It can easily be seen that the velocity of the jet has no significant influence on the sensor response. This DOE was performed using a window length of 0.2 inch (5 mm). Tests conducted with window sizes of 0.28 inch (7 mm) and 0.4 inch (10 mm) show the same result. From these results it can be concluded that the fiber does not produce enough drag force to strain the fiber, and thus it is not suitable for measuring velocity. However, it is thought that this concept could be further optimized as a temperature probe.

Single Sensor Flexible Beam

This concept shows an improved response to velocity in comparison with the open fiber. However, there is a significant influence from temperature. By compensating for temperature (for example, by using the open fiber sensor in combination with the single sensor flexible beam), an accurate velocity and temperature measurement could be achieved.

Differential Flexible Beam Sensor

As two fiber Bragg sensors are used in a differential setup in this concept the response from velocity is doubled.

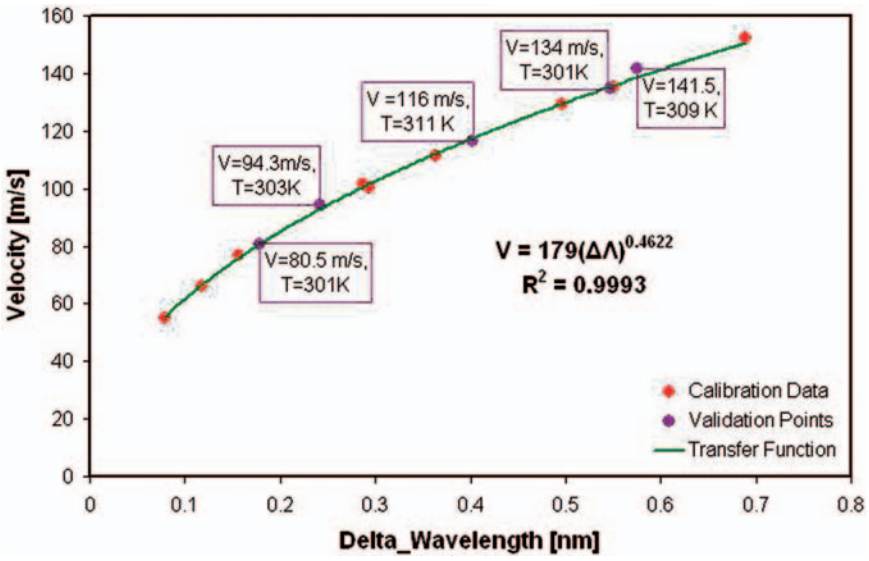

Figure 6. *Comparison of transfer function with validation points.*

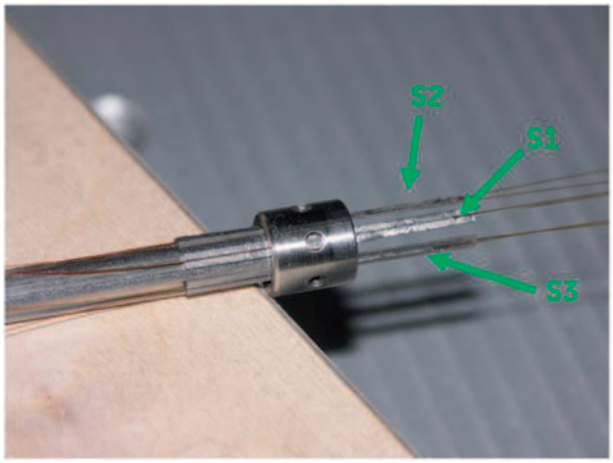

Figure 7. *Three-plate concept with three sensing elements.*

The temperature influence has become insignificant as the differential set-up compensates for temperature. The small response to temperature is thought to come from the temperature difference over the flexible beam, i.e., the tension sensor is exposed to the jet directly in contrast to the compression sensor. A probe manufactured from metal would reduce this influence. For a final application it should be taken into consideration to shield the fiber Braggs from the flow by incorporating them in the flexible beam.

Metal Differential Probe

It was decided to fabricate the probe design from metal. The previously described DOE was again performed. The accuracy of the transfer function was investigated in the next step. Figure 6 shows the transfer function calculated using the calibration points in the DOE compared with five validation points.

An average error of 1.2% was calculated between the actual values of the validation point and the calculated velocity through the transfer function.

VALIDATION OF THREE-PLATE PROBE

Multiple experiments were performed with the three-plate concept. Figure 7 shows the three-plate concept. Each flexible beam was mounted with two sensors in a differential set-up.

The test campaign was performed at the Politecnico di Milano (Technical University of Milan). The goal of this test campaign was to:

1. test the temperature insensitivity over a greater range;
2. validate the three-plate concept with measuring angles; and
3. determine the frequency response of the single metal probe.

The facility at which the tests were performed had the following specifications:

- Flow supply: Pressure vessel of 100 bar, filled overnight with reciprocating compressor.
- Capable of constant jet Mach 0.3 for 3–4 hours.
- Dimensions of the nozzle: 60 mm × 50 mm.
- Flow conditioned between pressure vessel and nozzle.
- Mach number range: up to 2.2 (continuously up to Mach 1).
- Temperature range: 285–340 K.
- Pressure accuracy approximately 0.5% of dynamic head.
- Angular accuracy approximately 0.15°.

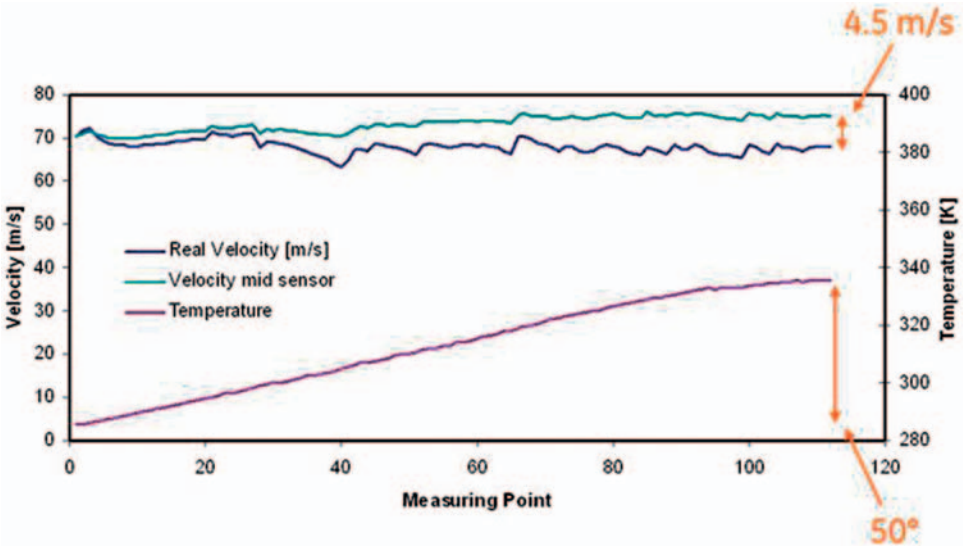

Figure 8. *Results from temperature sensitivity test.*

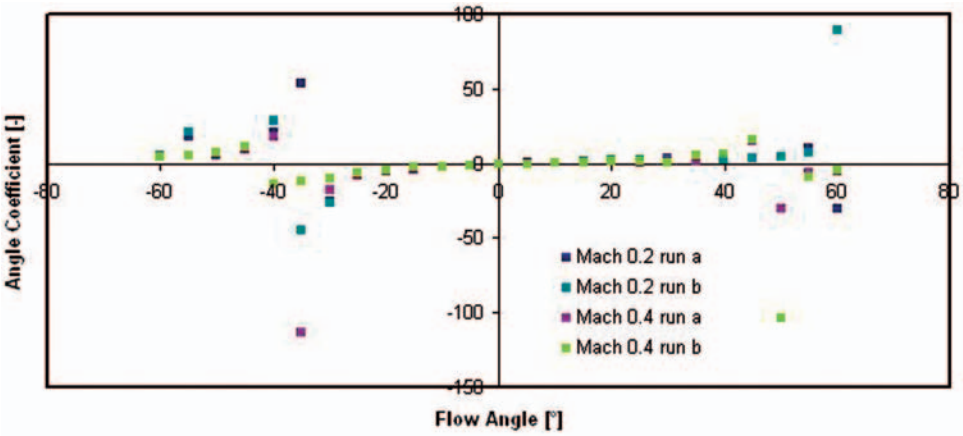

Figure 9. *Angle coefficient from −60° to +60° for Mach 0.2 and 0.4.*

Figure 8 presents the results from the temperature sensitivity test. The temperature was increased over a time period of 2 hours from 285 K to approximately 335 K.

It can been seen that with an increase of 50 K in the flow temperature an error of 14.8 feet/s (4.5 m/s) is induced on the read-out. This error can therefore be reduced by calibrating the sensor at the expected flow temperatures of the application.

The first test was performed by varying the relative angle of the probe to the jet from −60° to +60°. The three signals were combined in the following coefficient according to Dudzinski and Krause (1969), α:

$$\alpha = \frac{S_2 - S_3}{S_1 - {}^1/_3\,(S_1 + S_2 + S_3)}$$

where S_1 is the differential output of the two sensors on the middle plate, S_2 is the signal from the left plate, and S_3 is the signal from the right plate (see Figure 7). This coefficient is normally used as an input for the reduction methods for three-hole pneumatic probes. Figure 9 shows the results from these tests with a jet velocity of Mach 0.2 and 0.4 with a redundancy test for both Mach numbers. Two runs (a and b) were performed for redundancy.

It becomes clear that the sensor response is unstable outside the range −25° to +25°. This is due to the wake of one of the side sensing plates on the other sensing plates. This angle range is comparable to standard three-hole pneumatic probes. By adjusting the relative angle and position of the plates it is thought that this range can be extended. Figure 10 shows the results from the tests performed at angles from −25° to +25° and at Mach 0.3, 0.35, 0.4 and 0.5.

During the test it was discovered and confirmed by the results that one of the sensing elements had a

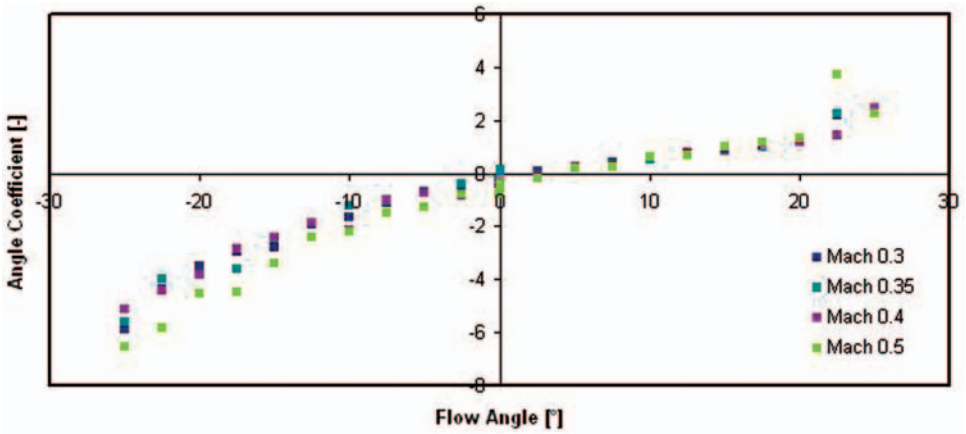

Figure 10. *Angle coefficient from −25° to +25° for Mach 0.3, 0.35, 0.4 and 0.5.*

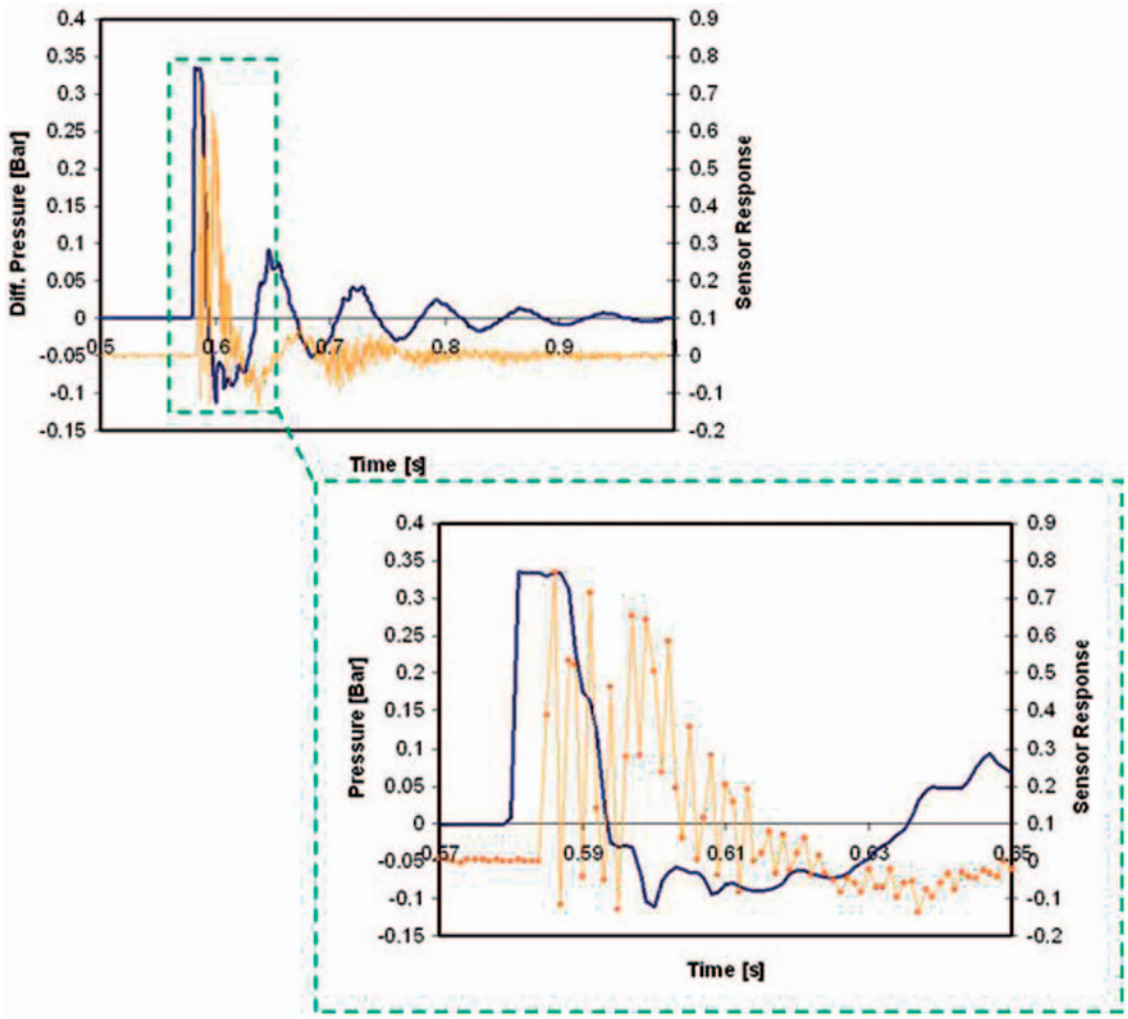

Figure 11. *Response of the probes to the shock wave.*

construction failure, causing the spread between −25° and 0°. The fiber became partially loose from the material and could not be repaired during the test campaign. However, a clear trend can be seen in the data from −25° to +25° and it can be concluded that the angle can be measured using the three-plate concept. Additional tests showed a repeatability of ±2°. However, with optimization of the plate position,

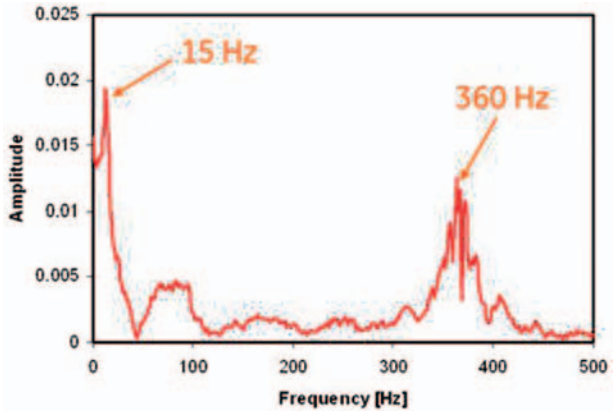

Figure 12. *Frequency spectra of fiber sensor response.*

relative angle and mechanical design of the probe, it is believed that the accuracy and repeatability can be increased significantly.

SHOCK TUBE TESTING

Shock tube experiments were performed to determine the frequency response of the single plate differential probe. A small chamber divided from the tube by a diaphragm was pressurized. By choosing the diaphragm burst pressure a controlled shockwave could be sent through the tube. The frequency response could be determined by comparing the response of the reference probe with that of the single plate probe. The diaphragms used during the experiment burst between 5 and 7 psi (350 and 500 mbar). Figure 11 shows the response of the probes at shock wave of 5 psi (350 mbar).

Figure 12 shows the spectra that can be calculated from the fiber sensor response. The plot shows two clear peaks in the frequency response. The 15 Hz peak is thought to be the "bulk" of the wave traveling by as this frequency also shows up in the response of the reference probe. The 360 Hz peak is the limit of the response of the sensor. The frequency response of the fiber sensor is much higher than that of the pneumatic probes. It should be emphasized that the frequency response does not change when the length of the fiber is increased, i.e., the interrogator can be placed at any arbitrary length from the sensor without impacting on the response. The results were repeated and confirmed with additional experiments.

CONCLUSION

Different concepts of flow sensors using fiber Bragg elements were tested and compared. Fiber Bragg sensors can be used to evaluate the velocity of a flow by correlating the strain induced by the flow over a beam. Also the paper shows that a differential arrangement of fiber Bragg sensors allows a reduction in the influence of temperature over the velocity measurement, and that the concept proposed can be used to determine the direction of the flow within a range of $\pm 25^{\circ}$. The proposed probe also provides a better frequency response, independent of the installation length required for the tubing/fiber optic, providing clear benefits compared with standard pneumatic probes.

ACKNOWLEDGMENTS

The authors gratefully acknowledge the technical support of Ray Chupp (GEE), Tom Farrell (GEE), Vivek Badami (GEE), Ted Furlong (GE Sensing), Scott Hoyte (GEE), Ken Moore (GEE), Tony Krull (GEE), Tim Healy (GEE), Axel Busboom, Hua Xia (GE GR), Lou Cerone, Keith Parker, Ralph Blakemore, and John Blanton (GEE). This work was funded under Internal Research and Development (IRD) funding. The authors gratefully acknowledge the financial support of GE Energy in this development effort.

REFERENCES

Botsis, J., Humbert, L., Colpo, F. and Giaccari, P. 2005. "Embedded Fiber Bragg Grating Sensor for Internal Strain Measurements in Polymeric Materials," *Optics and Lasers in Engineering*, 43:491–510.

Dudzinski, T.J. and Krause, L.N. 1969. "Flow Direction Measurement with Fixed Position Probes," *NASA TM X*, 1904.

Hill, K.O. and Meltz, G. 1997. "Fiber Bragg Grating Technology Fundamentals and Overview," *Journal of Lightwave Technology*, 15:1263.

Jin, L., Zhang, W., Zhang, H., Liu, B., Zhao, B., Tu, Q., Kai, G. and Dong, X. 2006. "An Embedded FBG Sensor for Simultaneous Measurement of Stress and Temperature," *IEEE Photonics Technology Letters*, 18:154.

Othonos, A. 1997. "Fiber Bragg Gratings," *Rev Sci Instrum*, 68: 4309–4341.

Rao, Y.-J. 1997. "In-fibre Bragg Grating Sensors," *Meas Sci Technol*, 8:355–375.

Udd, E. 1995. *Fiber Optic Smart Structures*, John Wiley & Sons, Inc, New York.

Zhao, Y., Chen, H. and Yang, J. 2005. "Novel Target Type Flowmeter Based on Differential Fiber Bragg Grating Sensor," *Elsevier Measurement*, 38:230–235.